

RESEARCH

Open Access



# Effect of three cannulated compression screws combined with an obstructing screw on the biomechanical performance of pauwels type III femoral neck fractures: a finite element analysis

Er-dan Huang<sup>1</sup>, Huo-huo Xue<sup>1\*†</sup>, Liang Chen<sup>2</sup>, Yang Feng<sup>1</sup>, Liang Zhao<sup>1</sup>, Zhi-Hui Zhong<sup>1</sup> and Ming Zheng<sup>1\*†</sup>

## Abstract

**Background** Obstructing screws (OS) are an effective surgical method for treating Pauwels type III femoral neck fractures. This study compared the mechanical properties of various surgical techniques for treating such fractures using finite element analysis.

**Methods** An ideal finite element model of the femur was established based on computed tomography scans of healthy individuals. Four internal fixation methods were designed: the three cannulated compression screws (3CCS) group, 3CCS + horizontal screw (3CCS + HS) group, 3CCS + OS (3CCS + OS) group, and 3CCS + medial buttress locking plate (3CCS + BL) group. The same pressure direction and magnitude were applied to observe the stress distribution in the femur under different surgical techniques.

**Results** The stress distribution, fracture displacement, and femoral stiffness varied across the internal fixation groups. The 3CCS + OS group exhibited the most balanced femoral stress distribution (126.49 MPa), effectively dispersing stress on the CCS. Its overall femoral stiffness (510.95 N/mm) and fracture displacement (4.11 mm) were second only to the 3CCS + BL group (554.09 N/mm, 3.79 mm) and significantly better than the 3CCS (441.18 N/mm, 4.76 mm) and 3CCS + HS (449.68 N/mm, 4.67 mm) groups.

**Conclusions** The combination of CCS and antishield OS demonstrated significant mechanical advantages and lower biological interference in the treatment of Pauwels type III femoral neck fractures. This method not only provides excellent mechanical stability but also ensures biological safety, offering benefits such as simplicity of operation, minimal invasiveness, and a low risk of complications. It holds great potential for widespread clinical application.

<sup>†</sup>Huo-Huo Xue and Ming Zheng contributed equally to this work.

\*Correspondence:

Huo-huo Xue  
xuehuohuo63@gmail.com  
Ming Zheng  
18150067268@163.com

Full list of author information is available at the end of the article



**Keywords** Obstructing screw, Pauwels type III femoral neck fractures, Finite element analysis

## Background

Femoral neck fractures are a common type of fracture encountered in clinical practice, with the Pauwels classification system widely used to differentiate between fracture types. In this system, angles of 30° and 50° serve as key thresholds. As the Pauwels angle increases, the shear force at the fracture site increases significantly [1, 2]. Pauwels type III fractures, characterized by a Pauwels angle of >50°, are more commonly observed in young and middle-aged adults following high-energy trauma. These fractures are highly unstable, with a substantial risk of fixation failure and a poor prognosis. Studies have shown that the nonunion rate for Pauwels type III fractures ranges from 16 to 59%, and the incidence of femoral head necrosis can be as high as 11–86% [3, 4].

Currently, cannulated screw fixation is the primary clinical method for treating Pauwels type III femoral neck fractures. Although cannulated compression screws (CCS) have demonstrated efficacy in some cases, the stability of this fixation remains controversial, especially in the presence of high shear forces. To improve fixation stability, some orthopedic surgeons have incorporated medial buttress locking plates (BL) in addition to CCS [5–7]. Although this approach has shown favorable clinical outcomes in certain cases, it has also generated concerns and controversies. The increased surgical trauma, higher anesthesia risks due to prolonged operation times, and the potential for postoperative complications are significant limitations [8, 9], which have restricted the broader adoption of this method.

Additionally, horizontal screws (HS) represent an improved fixation strategy proposed by our team for the treatment of Pauwels type III fractures. This approach was designed to counteract shear forces; however, its clinical efficacy remains highly debated [10, 11]. Consequently, the primary challenge in treating such fractures lies in achieving mechanical stability while minimizing surgical trauma and biological damage.

Based on the above background, we have introduced a new treatment strategy: incorporating an antishield obstructing screw (OS) into the standard CCS configuration (Fig. 1). The insertion method for the OS is similar to that of an HS. By positioning the screw head slightly above the fracture line, the shear forces at the fracture site can be converted into compressive stress, providing continuous compressive force at the fracture ends during healing. However, this new surgical approach has not yet undergone comprehensive mechanical testing for validation.

Finite element analysis (FEA) is a widely used numerical simulation method in both engineering and clinical

research. By simulating a femoral model and applying corresponding loads, FEA can replicate realistic microscopic mechanical scenarios. Therefore, in the present study, we employed FEA to calculate the micromechanics, providing theoretical support for this new surgical strategy.

## Methods

### Computed tomography (CT)

The research protocol was approved by the Ethics Committee of Fuzhou Second General Hospital (Approval No: 2021089). Written informed consent was obtained from the participant, and all methods adhered to relevant guidelines and regulations. This study is a biomechanical investigation, and no clinical trial registration number is applicable. The study participant was a healthy 30-year-old man (weight: 70 kg; height: 174 cm) with no history of femoral deformities, fractures, tumors, infections, other conditions, or trauma or surgery involving the femur. Imaging data were obtained from his normal, healthy left femur.

### Surgical procedures

After achieving satisfactory reduction of the femoral neck fracture, three CCS were routinely used for fixation. The first Kirschner wire was inserted through the lateral cortex of the subtrochanteric region, with the insertion point located at the intersection of the lower one-third of the lesser trochanter and the lateral cortex of the femur. The wire was directed parallel to the femoral calcar, forming a collo-diaphyseal angle of approximately 130° and an anteversion angle of approximately 15°, penetrating into the lower part of the femoral head. The other two Kirschner wires were inserted approximately 11 × 5 cm above the first wire in an inverted triangle pattern into the femoral neck, with a spacing of approximately 0.8–1 cm between the screws. The three guide wires were parallel to each other and distributed in the inverted triangle configuration.

Next, an OS was used for shear-resistant fixation. The fourth guide wire was inserted approximately 0.5 cm below the highest point of the external prominence of the greater trochanter, passing through the lateral cortex and directed toward the medial fracture line of the femoral neck, from outside to inside. It exited near the midpoint of the medial fracture line, with the exit point positioned near the center of the medial fracture line above the distal cortical bone. The final positioning ensured that the screw threads engaged the proximal medial cortex at the exit point. After measuring the guide wire length and reaming the canal, three 7 × 3 mm partially threaded CCS



**Fig. 1** X-ray imaging: cannulated compression screws combined with obstructing screw for the treatment of Pauwels type III femoral neck fractures

and one  $7 \times 3$  mm fully threaded headless OS were placed according to the measured lengths.

### Three-dimensional reconstruction model

CT was performed from the upper part of the iliac bone to the knee joint. Three-dimensional CT images of the femur were generated with a reconstruction thickness and interval of 1 mm and saved in DICOM format. The complete DICOM files were imported into Mimics 21.0 software (Materialise Company, Belgium), where threshold adjustments were made to remove soft tissue shadows and unnecessary bone structures. The “Calculate 3D” function was used to generate triangular surface geometric models, and the quality and quantity of the triangular surface mesh were adjusted to obtain a smooth three-dimensional image closely resembling the actual structure, which was then exported as an STL file. This STL file was subsequently imported into Geomagic Studio 2014 (Raindrop Company, USA) for surface fitting and smoothing. Precise surface modeling was used to generate a normal three-dimensional geometric model of the femur.

The femoral neck underwent reverse processing, generating a corresponding fracture body (thickness of 0.2 mm) based on the Pauwels type III fracture criteria ( $>70^\circ$ ). Four different internal fixation methods were designed: the three CCS (3CCS) group, 3CCS plus one HS (3CCS+HS) group, 3CCS plus one OS (3CCS+OS) group, and 3CCS plus a medial buttress locking plate (3CCS+BL) group (Fig. 2). The screws were simplified as cylinders, with appropriate friction coefficients

set to simulate the screw threads’ engagement with the bone structure. Among these, the outer diameter of the threaded section of the 3CCS, the outer diameter of the smooth section, and the inner diameter of the cannulated section were 7.3, 4.8, and 2.8 mm, respectively, with lengths determined according to the actual femur size. The size parameters of the HS were identical to those of the 3CCS, and it was implanted transversely into the femoral head. The OS was a variable cross-section screw, with minimum and maximum diameters of 6 and 7.5 mm, respectively, implanted into the femoral neck fracture location, with the thin end protruding a certain length. The BL system consisted of one titanium alloy plate and three small screws, with the plate bent to fit the inner side of the femoral neck; one small screw was positioned above the fracture line, and two were below it. The BL was 3 mm thick, 11 mm wide, and 75 mm long, and the diameter of the small screws was 4 mm, with lengths determined according to the actual femur size.

Based on material data from published literature [3–5, 12], the cortical bone, cancellous bone, screws, and BL were modeled as isotropic, homogeneous, and continuous linear elastic materials [4–7, 13] (Table 1). According to previous studies on contact settings [12, 14], the femoral neck fracture surface was modeled as completely fractured and nondisplaced, with the fracture surface assigned frictional contact and a friction coefficient of 0.46. Frictional contact was also established between the BL and bone surface, with a friction coefficient of 0.3, whereas the screw–bone contact interface was set as bonded to ensure the screws do not pull out.

### FEA

The final femur model, including the internal fixation models, was imported into MSC Nastran 2019 (NASA Company, USA) for computational analysis to examine the results. This phase primarily aimed to evaluate the biomechanical performance of different internal fixation methods, particularly their effect on the load-bearing capacity of the femur. Using finite element methods, simulations were conducted for the 3CCS, 3CCS+HS, 3CCS+OS, and 3CCS+BL groups. In addition to determining the stiffness of the femur, this analysis generated equivalent stress contour maps for the fracture surface and internal fixation screws as well as displacement contour maps for the entire femur and the fracture surface.

### Finite element meshing and convergence analysis

The geometric models corresponding to the normal, 3CCS, 3CCS+HS, 3CCS+OS, and 3CCS+BL groups were imported into Hypermesh 14.0 for meshing, and binary data format files were exported (Fig. 3). To ensure accurate data, a mesh convergence analysis was performed on the normal group to evaluate the effect of

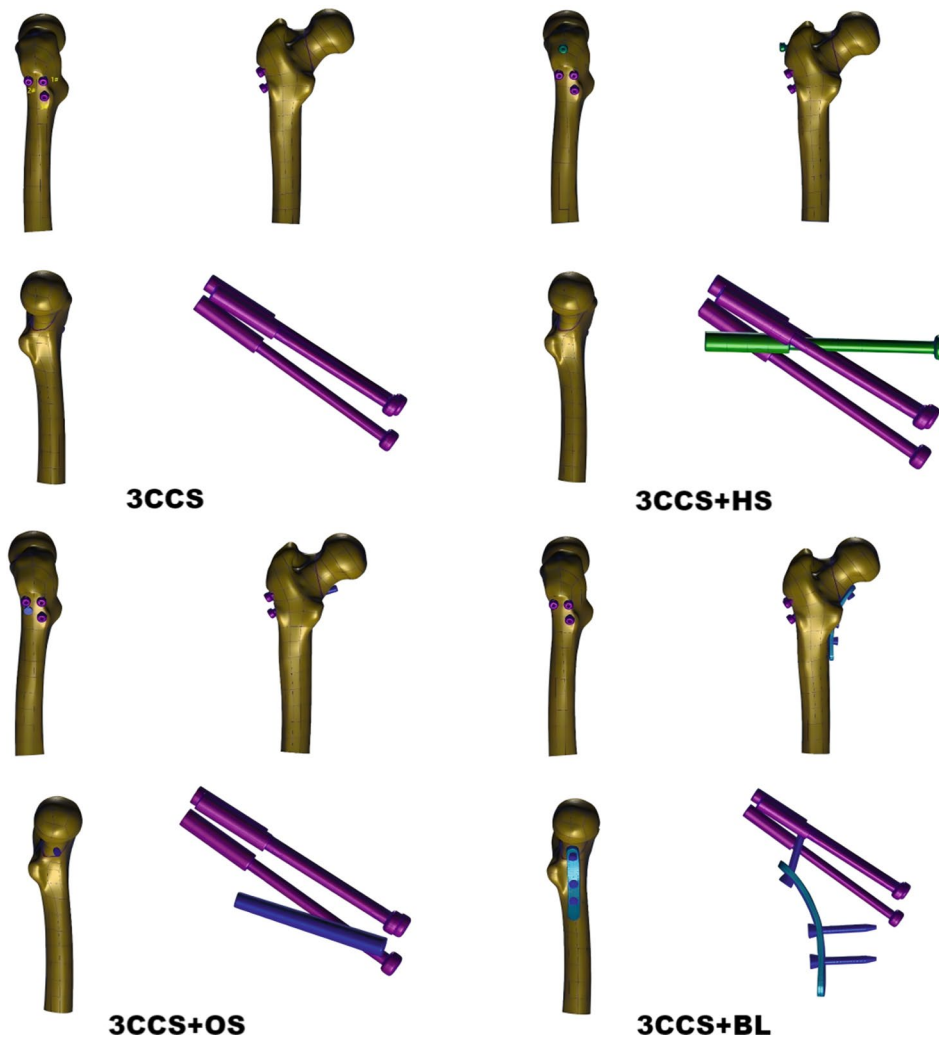


**Fig. 2** Four internal fixation methods were designed: (a) three cannulated compression screws (3CCS) group; (b) three cannulated compression screws (3CCS) + horizontal screw (HS) group; (c) three cannulated compression screws (3CCS) + obstructing screw (OS) group; (d) three cannulated compression screws (3CCS) + medial buttress locking plate (BL) group

**Table 1** Femoral structure and instrumentation material properties

Femoral structure and instrumentation	Young's modulus (MPa)	Poisson's ratio
Cortical bone of the femur	16,800	0.30
Cancellous bone of the femoral head	840	0.29
Cancellous bone of the femoral neck	620	0.29
Cancellous bone of the femoral trochanter	300	0.29
Cancellous bone of other regions	840	0.29
Internal fixation screws and plates (Ti-6Al-7Nb)	110,000	0.33

mesh size on the predictive results of the finite element model. Four different mesh sizes (2, 1.5, 1, and 0.5 mm) were tested, and the peak equivalent stress of the femoral head was compared. Based on this comparison, a final mesh size of 1 mm was selected, balancing shorter

computation time with the requirement that the variation in peak Von Mises stress remains < 5% (Table 2).

**Boundary conditions and loads**

Loading and boundary constraints were applied to each group's femoral model as follows. (1) Boundary constraints: All nodes at the distal end of the femur were fixed, restricting the degrees of freedom in all six directions. (2) Load application: Based on previously published literature [3, 15], the load on the femoral head during unilateral stance, due to the action of the abductors, can reach three times the body weight. Accordingly, a load of 2100 N was applied along the mechanical axis in the weight-bearing area of the femoral head to simulate the biomechanical characteristics experienced by a 70 kg individual during unilateral stance.

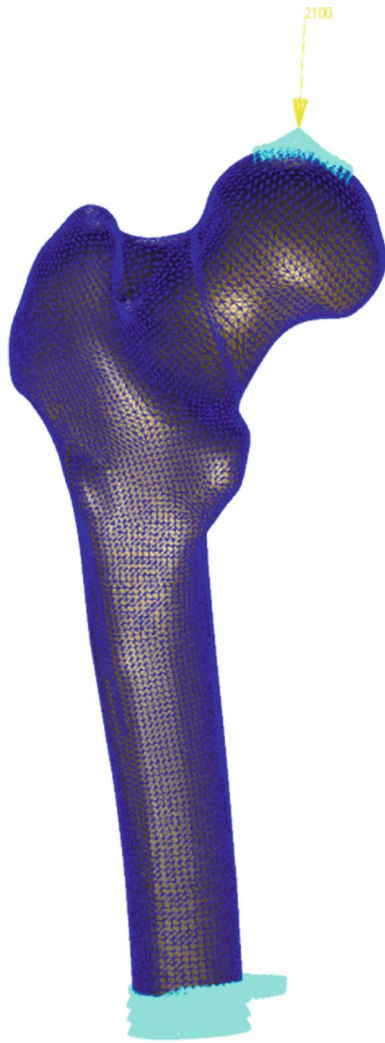


**Fig. 3** Load application and boundary constraint operations on the femoral model

**Table 2** Mesh convergence test results

Group	Element size (mm)	Nodes	Units	Percentage change in peak Von Mises stress
Reference model	0.5	227,970	1,378,287	-
Model A	1.0	43,757	230,988	< 5%
Model B	1.5	22,907	114,963	> 5%
Model C	2.0	16,638	82,344	> 5%

**Validity testing**

To verify the modeling method and the validity of the material parameter settings, boundary conditions, and model simplifications in the finite element simulation, a load analysis was performed on the normal femur model. By observing the distribution of equivalent, maximum principal, and minimum principal stresses, as well as the displacement cloud diagram, the following results

were obtained. The cortical bone on the medial and lateral sides of the femur experienced significant stress, with compressive stress on the medial side (peak value of approximately -67.89 MPa) and tensile stress on the lateral side (peak value of approximately 46.89 MPa). The absolute value of medial stress was greater than that of lateral stress (Fig. 4). The peak equivalent stress of the femoral structure, maximum deformation displacement, and overall structural stiffness were approximately 66.38 MPa, 4.06 mm, and 517.24 N/mm, respectively (Fig. 4). These results align with the findings of Peng [16], Cha [17], and Wang [18], indicating that the computational model of the normal femur is effective and accurate.

**Results**

**Model validation**

A comprehensive, nonpathological femur model was successfully established. Using the same interference method, the equivalent stress of the model was compared with findings from previous studies. This comparison confirmed the validity and reliability of the finite element model developed in this study, with the error remaining within a controllable range.

**FEA**

Using CT reconstruction technology, three-dimensional reconstruction of the femoral tissue structure was performed, and reverse engineering techniques were applied to construct internal fixation structures for different fixation methods. Five groups of femoral models were assembled: normal, 3CCS, 3CCS+HS, 3CCS+OS, and 3CCS+BL. Stress and displacement analyses were then conducted on these models in a single-leg standing position using the finite element method (Figs. 5 and 6), with the 3CCS model serving as the reference for percentage increment calculations.

**Comparison of peak stress in the femur and internal fixation devices**

In the 3CCS group, the peak stress in the femur was 296.55 MPa. In the 3CCS+HS group, the peak stress decreased to 258.15 MPa (-12.95%). The 3CCS+OS group showed a significant reduction in femoral peak stress to 126.49 MPa (-57.35%), whereas the 3CCS+BL group exhibited an increase in peak stress to 311.16 MPa (+4.93%). For the internal fixation screws, the peak stress of CCS (1#) in the 3CCS group was 433.98 MPa, which decreased to 352.98 MPa (-18.66%) in the 3CCS+HS group. In the 3CCS+OS group, the peak stress for CCS (1#) decreased significantly to 136.03 MPa (-68.66%), further decreased to 108.90 MPa (-68.16%) for CCS (2#), and decreased to 72.24 MPa (-82.75%) for CCS (3#). In the 3CCS+BL group, the peak stresses for CCS (1#) and

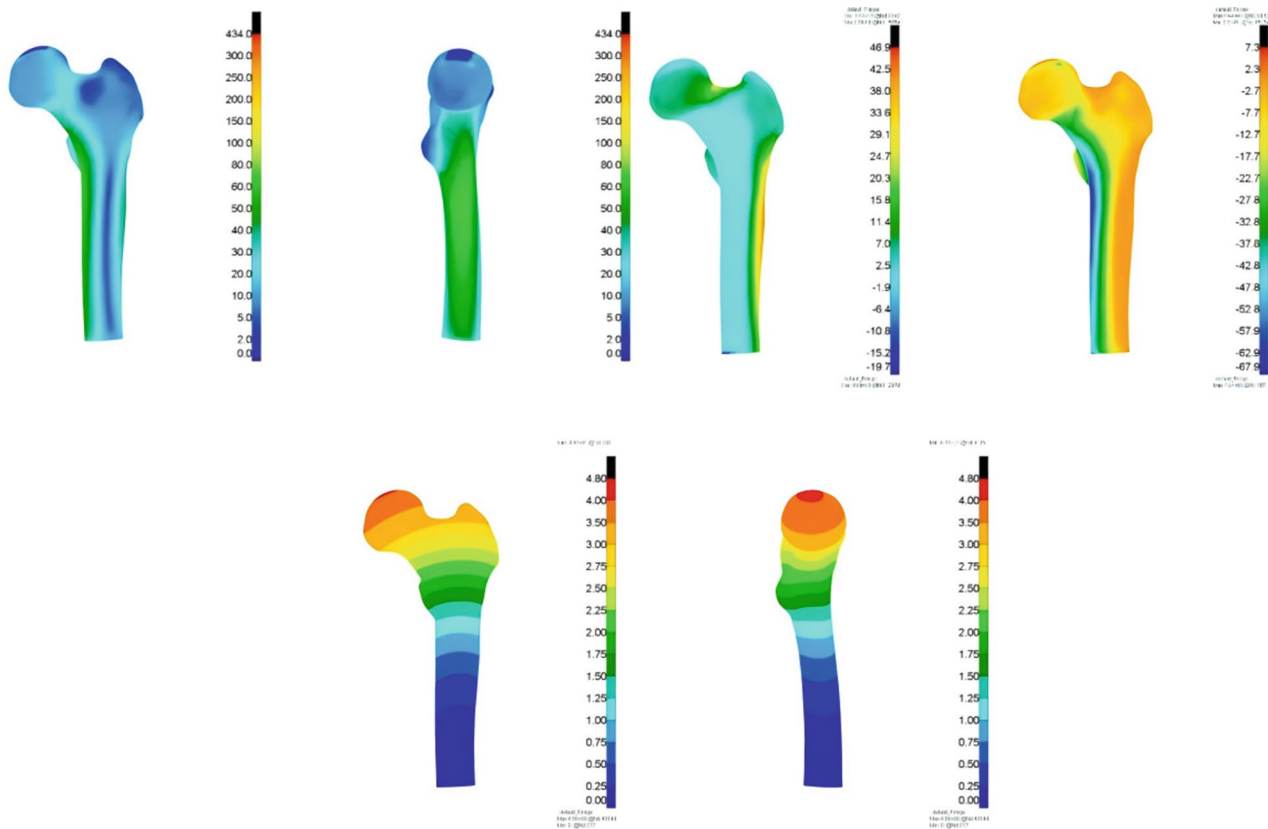


**Fig. 4** Validity tests indicate that the mechanical properties of the model in this study are comparable to those of previously established models

CCS (2#) were 101.76 MPa (−76.55%) and 99.06 MPa (−71.04%), respectively, demonstrating the effectiveness of BL in reducing stress on the surrounding internal fixation devices (Table 3; Fig. 7).

#### Comparison of the overall displacement of the femur and displacement at the fracture site

Analysis of the overall displacement of the femur and the relative displacement at the fracture site using different internal fixation methods showed that in the 3CCS group, the peak overall displacement and fracture site displacement were 4.76 and 1.53 mm, respectively. In the 3CCS+HS group, these values were 4.67 mm (−1.89%) and 1.48 mm (−3.27%), respectively, indicating that adding HS did not significantly improve femoral stability. Conversely, in the 3CCS+OS group, the overall displacement decreased significantly to 4.11 mm (−13.66%) and the relative displacement decreased to 1.14 mm (−25.49%), demonstrating the effectiveness of OS in limiting fracture displacement. The 3CCS+BL group exhibited the highest stability, with the overall displacement decreased to 3.79 mm (−20.38%) and the relative displacement decreased to 1.01 mm (−33.99%) (Table 4; Fig. 8).

#### Comparison of the overall stiffness of the femur

Regarding the comparison of the overall stiffness of the femur, the stiffness in the 3CCS group was 441.18 N/mm. With the addition of an HS, the stiffness slightly increased to 449.68 N/mm (+1.93%), indicating a minor enhancement in the overall structural stiffness due to the HS. In the 3CCS+OS group, the stiffness increased significantly to 510.95 N/mm (+15.81%), demonstrating the advantage of OS in improving fracture fixation. The 3CCS+BL group exhibited the highest stiffness, with a value of 554.09 N/mm (+25.59%) (Table 5; Fig. 9).

#### Discussion

Pauwels type III femoral neck fractures are highly unstable and carry a significantly higher risk of complications and fracture nonunion due to their unique anatomical location and large Pauwels angle [19–22]. This fracture type poses considerable challenges in clinical treatment. Conventional treatment typically involves fixation with 3CCS after fracture reduction. However, in practice, loss of reduction and internal fixation failure are common, which can result in treatment failure and poor prognosis [23–25]. In a previous study involving 122 postoperative fracture samples, 39 patients with 3CCS fixation experienced fracture nonunion [26]. This finding confirms that 3CCS cannot effectively counteract vertical shear forces.

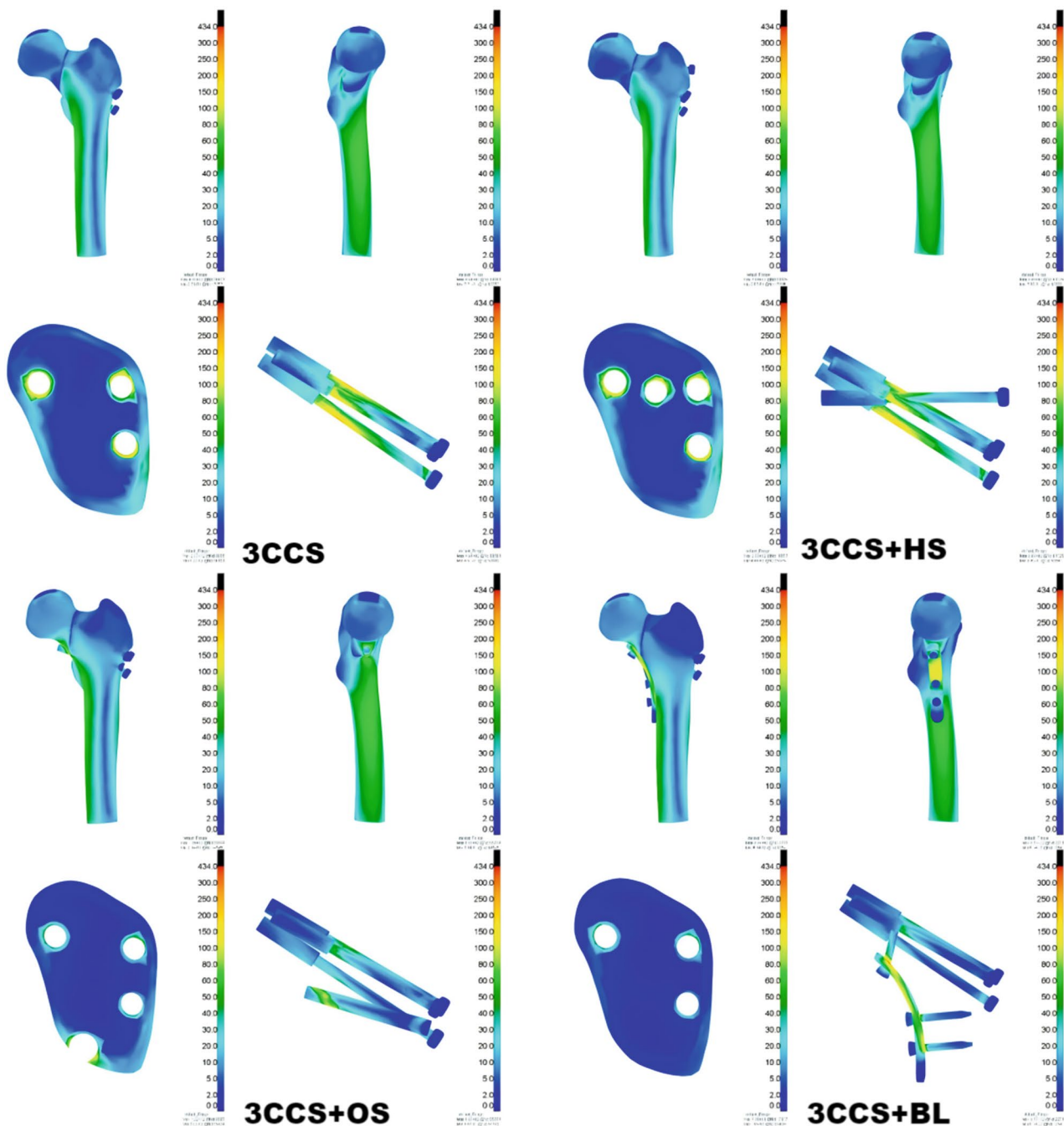


**Fig. 5** Stress characteristics of the four groups under different surgical conditions

In the present study, comparison of different fixation methods revealed that the BL fixation method combined with CCS demonstrated the best performance in terms of axial compression stiffness and provided the strongest mechanical stability. This finding has also been corroborated by other studies [27, 28]. The second most effective method was the antishear OS combined with CCS, whereas the fixation effect of the HS combined with CCS was relatively weak.

Although the BL provided the best mechanical stability and has been widely used in the past [29], its disadvantages cannot be ignored. The blood supply to the femoral head and neck primarily depends on the medial and lateral femoral circumflex arteries, particularly the medial femoral circumflex artery. Pauwels type III fractures are typically located below or involve the femoral head, and the fracture line may cross the joint capsule, increasing the risk of injury to critical blood vessels such as the superior and lateral metaphyseal arteries. When using

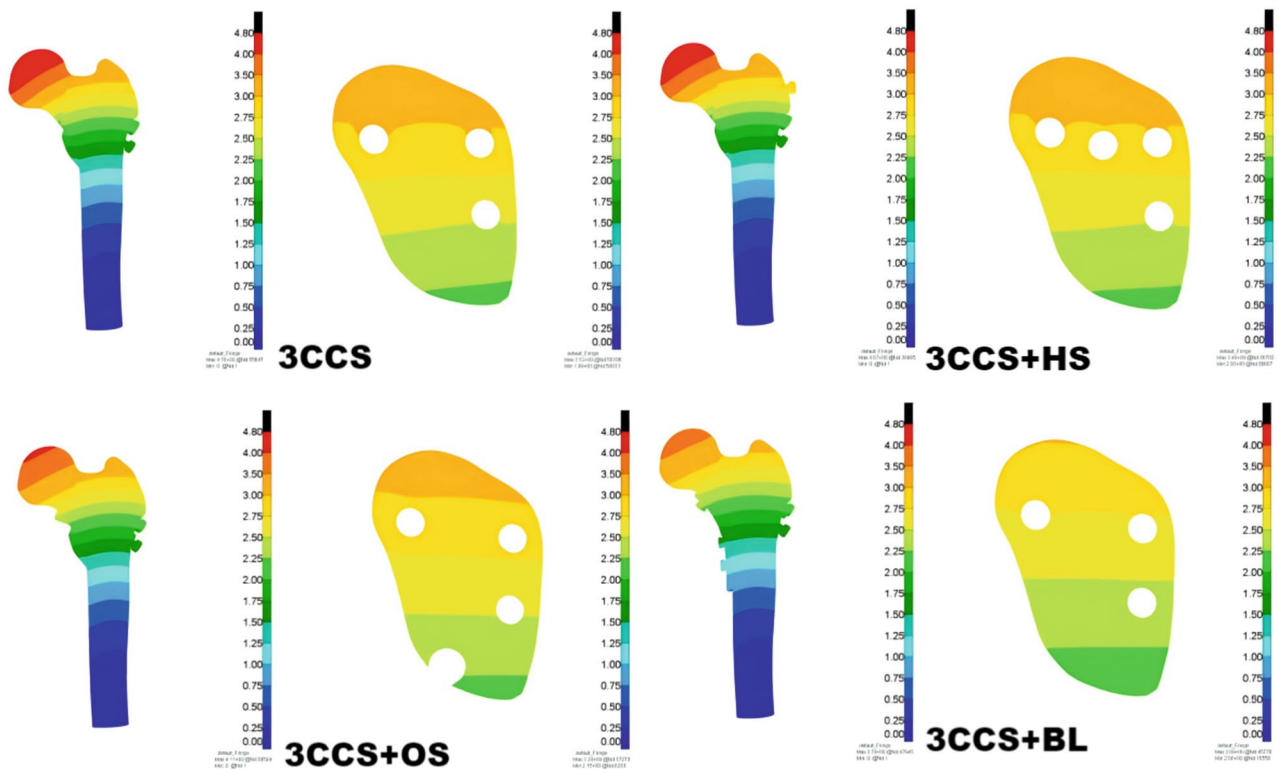


**Fig. 6** Overall femoral displacement and fracture end displacement characteristics of the four groups under different surgical conditions

**Table 3** Peak von mises equivalent stress of the femur and internal fixation devices (MPa)

	3CCS	3CCS+HS	3CCS+OS	3CCS+BL
Femur	296.55	258.15	126.49	311.16
Cannulated compression screw #1	433.98	352.98	136.03	101.76
Cannulated compression screw #2	342.00	323.62	108.90	99.06
Cannulated compression screw #3	418.71	388.52	72.24	53.30
Horizontal screw	/	241.79	/	/
Obstructing screw	/	/	127.69	/
Medial buttress locking plate	/	/	/	336.60

the BL, the medial hip incision must be extended, further aggravating injury to the circumflex femoral artery and increasing the likelihood of fracture nonunion or femoral head necrosis [28, 30]. In a meta-analysis involving 409 samples, a comparison between 3CCS and 3CCS+BL

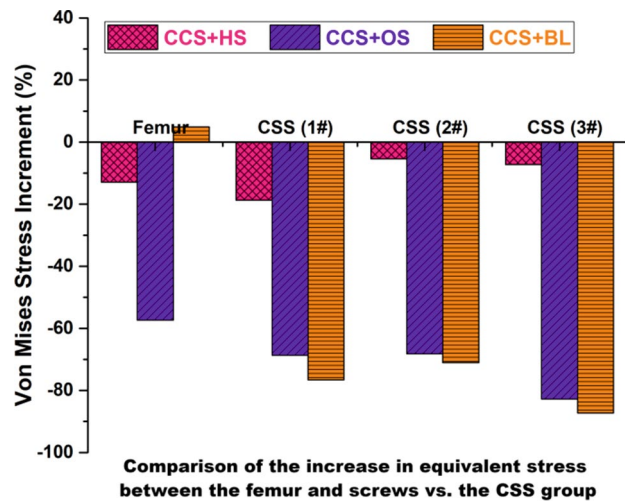


**Fig. 7** Comparison of the increase in equivalent stress between the femur and screws relative to the 3CCS group

**Table 4** Peak overall femoral displacement and relative fracture surface displacement and percentage increase relative to the 3CCS group

		3CCS	3CCS+HS	3CCS+OS	3CCS+BL
Peak displacement (mm)	Overall femoral displacement	4.76	4.67	4.11	3.79
	Relative displacement of the fracture surface	1.53	1.48	1.14	1.01
Percentage increase (%)	Overall femoral displacement	1.0	-1.89	-13.66	-20.38
	Relative displacement of the fracture surface	1.0	-3.27	-25.49	-33.99

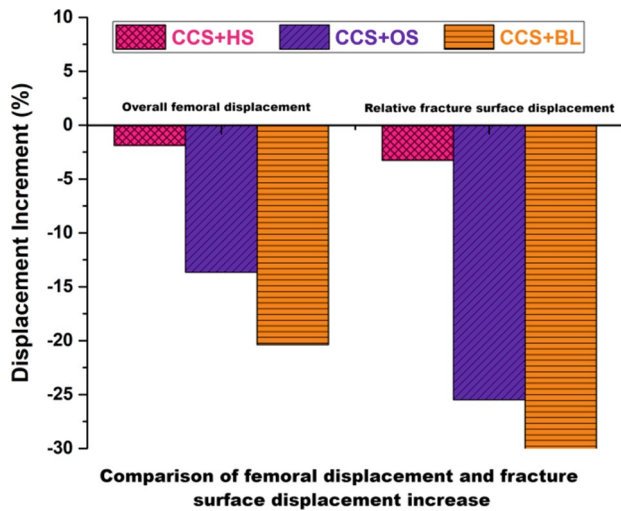


**Fig. 8** Comparison of femoral displacement and fracture surface displacement increase

**Table 5** Overall femoral stiffness

	3CCS	3CCS+HS	3CCS+OS	3CCS+BL
Stiffness (N/mm)	441.18	449.68	510.95	554.09
Percentage increase relative to the 3CCS group (%)	1.0	1.93	15.81	25.59

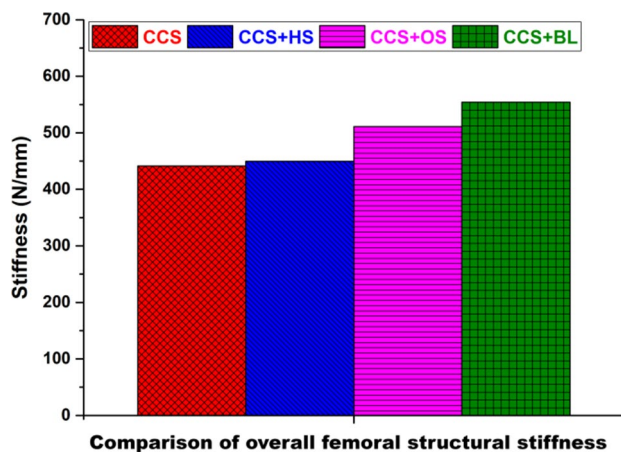


**Fig. 9** Comparison of overall femoral structural stiffness

surgical methods revealed that the BL group experienced greater blood loss (mean difference [MD] = 23.05, 95% confidence interval [CI] = 13.86–32.24) and longer surgery times (MD = 23.05, 95% CI = 13.86–32.24) [31]. These factors warrant careful consideration when selecting this method.

Conversely, although the 3CCS+HS group included an additional HS for shear resistance compared with the 3CCS group, the results of this study indicated that the improvement was not significant. Furthermore, the longitudinal shear force can easily cause swing displacement, using the screw cap as the fulcrum, which may

result in fixation failure. Consequently, the effectiveness of this method is limited [11, 28].

To improve the fixation of Pauwels type III femoral neck fractures, an improved fixation method was proposed in this study. Based on the 3CCS method, antishear OS were implanted at the fracture line of the medial scalar of the femur. These screws, partially embedded into the hard bone of the scalar cortex of the femur through their threads, effectively resisted the shear force at the fracture site and converted it into compressive stress. This conversion provided sustained compressive stress during fracture healing and facilitated the sliding compression of the cannulated screw throughout the healing process. This method provides a more stable internal fixation solution while preserving a good blood supply to the femoral head.

FEA revealed that compared with the 3CCS group, the peak stress of the femur in the 3CCS+OS group decreased by 57.35%, indicating a significant reduction in load bearing. Additionally, stress evaluation of the internal fixation screws reflected a substantial decrease, with the peak stress of CCS #1, 2, and 3 decreasing by 68.66%, 68.16%, and 82.75%, respectively. These results demonstrate that the stability of the internal fixation is significantly improved when external forces are applied. Furthermore, the overall femur displacement decreased by 13.66%, and the relative displacement decreased by 25.49%, indicating enhanced stability at the fracture site. The overall stiffness increased by 15.81%, indicating enhanced femoral stability following 3CCS+OS treatment, which contributed to better bone support and healing. These findings strongly support the effectiveness of 3CCS+OS therapy.

**Limitations**

In this study, FEA of 3CCS+OS provided valuable insights into femur stress and displacement; however, some limitations remain. First, to simplify the model, the homogeneous material assumption was used, and the heterogeneity of bones and the actual characteristics of different structures were not fully considered. This may lead to differences between the results of the stress distribution and the actual situation. Additionally, the properties of the materials used in this study were all linear, which was inconsistent with the nonlinear properties of actual bones under different loading conditions, potentially affecting the accuracy of the stress assessment. Second, the construction of the model was based on the anatomy of a specific patient, and this individual variation may significantly influence the results, limiting its applicability to a broader population. Furthermore, this study only simulated femur stress and displacement under specific conditions and did not account for the potential effects of multiple influencing factors, such as biomechanical

load changes, patient activity levels, and femur rotation, on the results. Furthermore, this study did not evaluate the impact of different fracture line angles on the stability of screw fixation, as it only modeled a Pauwels type III fracture line with a single angle (71°). There may, in fact, be a close relationship between OS and specific fracture line angles, which was not explored in this study. Finally, due to funding limitations, the dynamic hip screw was not included for horizontal comparison. This omission, despite the dynamic hip screw's relatively reliable anti-fracture displacement effect, introduced some shortcomings in the conclusions. Therefore, further studies should consider more individual differences and include a broader range of surgical protocols to more accurately evaluate the effectiveness and stability of the 3CCS + OS technology in clinical applications.

## Conclusions

The fixation method combining CCS with OS demonstrated significant mechanical advantages and reduced biological interference in the treatment of Pauwels type III femoral neck fractures. This approach not only provides excellent mechanical stability but also ensures biological safety. It is easy to perform, minimally invasive, and associated with a low risk of complications, highlighting its broad potential for clinical application. Therefore, the fixation method of CCS combined with OS is worthy of further promotion and application in clinical practice to improve treatment outcomes for patients with femoral neck fractures.

## Abbreviations

CT	Computed tomography
FEA	Finite element analysis
CCS	Cannulated compression screws
3CCS	Three cannulated compression screws
HS	Horizontal screw
OS	Obstructing screw
BL	Medial buttress locking plate
MD	Mean difference
CI	Confidence interval

## Acknowledgements

We extend our thanks to the Fuzhou Second General Hospital for their assistance and collaboration.

## Author contributions

MZ and HHX contributed equally to this study. MZ, HHX designed the method. HHX, EDH designed the illustrations. LC, YF, LZ, ZHZ collected the relevant imaging data and translated the manuscript. All authors read and approved the final manuscript.

## Funding

This study was supported by the Fujian Provincial Clinical Medical Research Center for First Aid and Rehabilitation in Orthopedic Trauma (Grant No. 2020Y2014).

## Data availability

The dataset and materials generated and analyzed during the current study are available from the corresponding author on reasonable request.

## Declarations

### Ethics approval and consent to participate

Institutional review board approval was obtained from the ethics committee of Fuzhou Second General Hospital (Ethical Approval Number: 2021089). The volunteer participating in this study provided written informed consent. This study is biomechanical research, and no clinical trial registration number is applicable.

### Consent for publication

All personal information, images, and videos used in this study were obtained with the volunteer's written informed consent for publication.

### Competing interests

The authors declare no competing interests.

### Author details

<sup>1</sup>Fuzhou Second General Hospital, Fuzhou 350007, China

<sup>2</sup>The First Affiliated Hospital of Fujian Medical, Fuzhou 350007, China

Received: 3 November 2024 / Accepted: 23 April 2025

Published online: 15 May 2025

## References

- Luttrell K, Beltran M, Collinge CA. Preoperative decision making in the treatment of high-angle vertical femoral neck fractures in young adult patients. *J Orthop Trauma*. 2014;28:e221–5.
- Freitas A, Toledo Júnior JV, Ferreira Dos Santos A, Aquino RJ, Leão VN, Péricles de Alcântara W. Biomechanical study of different internal fixations in Pauwels type III femoral neck fracture - A finite elements analysis. *J Clin Orthop Trauma*. 2021;14:145–50.
- Li J, Zhao Z, Yin P, Zhang L, Tang P. Comparison of three different internal fixation implants in treatment of femoral neck fracture—a finite element analysis. *J Orthop Surg Res*. 2019;14:76.
- Gardner MP, Chong ACM, Pollock AG, Wooley PH. Mechanical evaluation of large-size fourth-generation composite femur and tibia models. *Ann Biomed Eng*. 2010;38:613–20.
- Grassi L, Väänänen SP, Amin Yavari S, Weinans H, Jurvelin JS, Zadpoor AA, et al. Experimental validation of finite element model for proximal composite femur using optical measurements. *J Mech Behav Biomed*. 2013;21:86–94.
- Heiner AD. Structural properties of fourth-generation composite femurs and tibias. *J Biomech*. 2008;41:3282–4.
- Mei J, Liu S, Jia G, Cui X, Jiang C, Ou Y. Finite element analysis of the effect of cannulated screw placement and drilling frequency on femoral neck fracture fixation. *Injury*. 2014;45:2045–50.
- Yildirim C, Demirel M, Karahan G, Cetinkaya E, Misir A, Yamak F, et al. Biomechanical comparison of four different fixation methods in the management of Pauwels type III femoral neck fractures: is there a clear winner? *Injury*. 2022;53:3124–9.
- Nwankwo CD, Schimoler P, Greco V, Kharlamov A, Westrick ER, Miller MC. Medial plating of Pauwels type III femoral neck fractures decreases shear and angular displacement compared with a derotational screw. *J Orthop Trauma*. 2020;34:639–43.
- Giordano V, Alves DD, Paes RP, Amaral AB, Giordano M, Belangero W, et al. The role of the medial plate for Pauwels type III femoral neck fracture: a comparative mechanical study using two fixations with cannulated screws. *J Exp Orthop*. 2019;6:18.
- Boraiah S, Paul O, Hammoud S, Gardner MJ, Helfet DL, Lorich DG. Predictable healing of femoral neck fractures treated with intraoperative compression and length-stable implants. *J Trauma Injury Infect Crit Care*. 2010;69:142–7.
- Stoffel K, Zderic I, Gras F, Sommer C, Eberli U, Mueller D, et al. Biomechanical evaluation of the femoral neck system in unstable Pauwels III femoral neck fractures: a comparison with the dynamic hip screw and cannulated screws. *J Orthop Trauma*. 2017;31:131–7.
- Wirtz DC, Pandorf T, Portheine F, Radermacher K, Schiffrs N, Prescher A, et al. Concept and development of an orthotropic FE model of the proximal femur. *J Biomech*. 2003;36:289–93.
- Chen W-P, Tai C-L, Shih C-H, Hsieh P-H, Leou M-C, Lee MS. Selection of fixation devices in proximal femur rotational osteotomy: clinical complications and finite element analysis. *Clin Biomech*. 2004;19:255–62.

15. Xia Y, Zhang W, Hu H, Yan L, Zhan S, Wang J. Biomechanical study of two alternative methods for the treatment of vertical femoral neck fractures - A finite element analysis. *Comput Meth Prog Bio*. 2021;211:106409.
16. Peng MJ-Q, Xu H, Chen H-Y, Lin Z, Li X, Shen C, et al. Biomechanical analysis for five fixation techniques of Pauwels-III fracture by finite element modeling. *Comput Meth Prog Bio*. 2020;193:105491.
17. Cha Y, Chung JY, Jung C-H, Kim J-W, Lee J, Yoo J-I, et al. Pre-sliding of femoral neck system improves fixation stability in Pauwels type III femoral neck fracture: a finite element analysis. *BMC Musculoskelet Disord*. 2023;24:506.
18. Wang G, Tang Y, Wu X, Yang H. Finite element analysis of a new plate for Pauwels type III femoral neck fractures. *J Int Med Res*. 2020;48:300060520903669.
19. Lin H, Lai C, Zhou Z, Wang C, Yu X. Femoral neck system vs. four cannulated screws in the treatment of Pauwels III femoral neck fracture. *J Orthop Sci*. 2023;28:1373–8.
20. Yin B-H, Liu C-J, Sherrier MC, Sun H, Zhang W. Compressive buttress compared with off-axial screw fixation for vertical femoral neck fractures in young adults: a prospective, randomized controlled trial. *J Orthop Surg Res*. 2024;19:42.
21. Wen Q, Gu F, Su Z, Zhang K, Xie X, Li J, et al. Gamma nail combined with one cannulated compression screw fixation for treating Pauwels type III femoral neck fractures in young and middle-aged adults: clinical follow-up and Biomechanical studies. *Orthop Surg*. 2023;15:1045–52.
22. Steffensmeier A, Shah N, Archdeacon M, Watson D, Sanders RW, Sagi HC. Clinical and Biomechanical effects of femoral neck buttress plate used for vertical femoral neck fractures. *Injury*. 2022;53:1137–43.
23. Lee DH, Kwon JH, Kim K-C. The effects and risk factors of femoral neck shortening after internal fixation of femoral neck fractures. *Clin Orthop Surg*. 2024;16:718.
24. Zhang Y, Yan C, Zhang L, Zhang W, Wang G. Comparison of ordinary cannulated compression screw and double-head cannulated compression screw fixation in vertical femoral neck fractures. *BioMed Res Int*. 2020;2020:1–9.
25. Liu J, Li Z, Ding J, Huang B, Piao C. Biomechanical analysis of two medial buttress plate fixation methods to treat Pauwels type III femoral neck fractures. *BMC Musculoskelet Disord*. 2022;23:49.
26. Duckworth AD, Bennet SJ, Aderinto J, Keating JF. Fixation of intracapsular fractures of the femoral neck in young patients: risk factors for failure. *J Bone Joint Surg Br*. 2011;93:811–6.
27. Ma C, Liu Y, Liu J, Chen L, Huang J, Luo X, et al. The role of the medial buttress plate in the treatment of Pauwels type II and III femoral neck fracture in nonelderly patients: a retrospective study and preliminary results. *BMC Musculoskelet Disord*. 2022;23:100.
28. Liu Y, Zhao D, Wang W, Zhang Y, Wang B, Li Z. Efficacy of core decompression for treatment of canine femoral head osteonecrosis induced by arterial ischaemia and venous congestion. *HIP Int*. 2017;27:406–11.
29. Kunapuli SC, Schramski MJ, Lee AS, Popovich JM, Cholewicki J, Reeves NP, et al. Biomechanical analysis of augmented plate fixation for the treatment of vertical shear femoral neck fractures. *J Orthop Trauma*. 2015;29:144–50.
30. Hu Y, Yang Q, Zhang J, Peng Y, Guang Q, Li K. Methods to predict osteonecrosis of femoral head after femoral neck fracture: a systematic review of the literature. *J Orthop Surg Res*. 2023;18:377.
31. Su Z, Liang L, Hao Y. Medial femoral plate with cannulated screw for Pauwels type III femoral neck fracture: a meta-analysis. *J Back Musculoskelet Rehabil*. 2021;34:169–77.

### Publisher's note

Springer Nature remains neutral with regard to jurisdictional claims in published maps and institutional affiliations.